JOINT INSTITUTE FOR NUCLEAR RESEARCH

FLEROV LABORATORY OF NUCLEAR REACTIONS

WAVE 7 – 13 JUNE TO 22 JULY, 2022

DETERMINATION OF MASSES OF THE SUPER HEAVY ELEMENTS IN THE EXPERIMENTS ON SYNTHESIS OF Cn AND Fn USING THE REACTIONS $^{48}Ca + ^{242}Pu$ AND $^{48}Ca + ^{244}Pu$

STUDENT :: SANCIA MORRIS

Institute of Chemical Technology, Mumbai, Indian Oil Campus, Bhubaneswar, Odisha, India.

SUPERVISOR :: VEDENEEV VIACHESLAV YURIEVICH

Flerov Laboratory of Nuclear Reactions

ABSTRACT

The Mass Analyser of Super Heavy Atoms or simply MASHA, is a device used to separate atoms according to their masses, which in turn lead to their identification. It is used mainly in the production and identification of Super Heavy Elements (SHE) by their mass to charge ratio. Usage of the well-known (ISOL) method to measure the masses of the produced nuclei online has been done as it is necessary for the measurement of short-lived isotopes of super heavy elements. In the present work, mass measurement and determination of isotopes of Hg have been performed, as it is a homologue to the SHEs: Cn and Fl. This may open the doors to new SHEs which are relatively stable and evidence to the existence of the so called “Island of Stability”.

MASHA was built for identification of super heavy elements (SHE) by their mass-to-charge ratios. The yields of SHE in full fusion reactions $^{48}Ca + ^{242}Pu$, $^{48}Ca + ^{244}Pu$ is very low due to its low cross-sections of several nanobarns. That is why the reactions of Hg formations as the possible homologue of 112 and 114 were used for the test experiments. The separation efficiency of mercury could predict the separation efficiency of super heavy elements and therefore predict its expected yields.

Contents

Introduction……..4

- **Joint Institute for Nuclear Research - JINR……5**
- **Flerov Laboratory of Nuclear Reactions - FLNR……..5**
- **Super Heavy Elements – SHE……..6**

MASHA……7

- **Mass Analyser of Super Heavy Atoms - MASHA……7**
- **MASHA - Setup of the instrument……8**
  - **Ion Source……8**
  - **Target Assembly and a Hot Catcher……9**
  - **Detector……9**
  - **Data Acquisition System……..10**

Method of operation……11

Task ……12

- **Discussion……12**

Detailed Discussions and Results……..14

- **Argon - 40 beam and Samarium - 148 target……14**
- **Argon-40 beam and Erbium-166 target……18**
- **Calcium-48 beam and Plutonium-242 target……22**

Conclusion……26

Acknowledgements……..26

References……..27

1. INTRODUCTION

The synthesis of super heavy elements that make up the so-called "island of stability" is a one of the main task of modern physics. Researchers are interested in investigation of heavy elements due to their shell effects, which cause them to be remarkably stable. For synthesis of stable heavy nucleus, it is necessary to introduce as many neutrons as possible into it. Inasmuch neutrons have no electric charge, it allow them go inside the nucleus without impediments of electromagnetic forces, thus, making neutrons a great construction nucleons of an atomic cores. To create the nucleus of a new element, the interacting cores of the projectile and target must merge with each other, become a one. To do this, it is needed to get close enough to each other that short-range nuclear forces became to act, in other words, there is a strong interaction. Now scientists collide two heavy nuclei, expecting outcome of impact will be a core of total mass. To conduct experiment, one of nuclei should be accelerated to a speed of about 0.1 of the speed of light using a heavy ion accelerator. All super heavy elements were obtained such way. Recent syntheses of super heavy elements (SHE) upwards with Z = 113 revealed nuclei with relatively long lifetimes (> 1 s) that can be chemically identified and characterized. The considerable increase in the stability of SHE points toward an initial confirmation of the existence of the island of stability. It behoves to emphasize the island of stability is located in the region of neutron-excess super heavy nuclei, therefore, the target and beam nuclei must also contain excess of neutrons. Having received a beam of calcium of the required intensity, experimentalists irradiate plutonium target. If, as result of the fusion of two nuclei, atoms of new elements are formed, it should escape from target and continue moving forward together with the beam. However, it must be separated from the initial beam and other reaction products. This function is performed by the separator. Basic problem of this research is low reaction cross-section of SHE with the complex of low total efficiency, which leads to a production rate of about one atom per week of bombardment. So, more powerful accelerators are being created at the moment to increase the yields of SHEs. The choice of α radioactive Hg is justified by the predicted shared chemical and physical properties of the two with elements Z = 112 and Z = 114. While the extrapolation of those properties to SHE is vulnerable to inaccuracies due to pronounced relativistic effects, it can nevertheless provide a good enough approximation for the behaviour of Cn and Fl inside the mass separator.

1.1 Joint Institute for Nuclear Research - JINR

The Joint Institute for Nuclear Research (JINR), in Dubna, Moscow Oblast (110 km north of Moscow), Russia, is an international research center for nuclear sciences, with 1200 researchers including 1000 Ph.Ds from eighteen countries, like Armenia, Azerbaijan, Belarus, Kazakhstan and Ukraine, members of the institution. The institute has seven laboratories, each with its own specialisation: theoretical physics, high energy physics (particle physics), heavy ion physics, condensed matter physics, nuclear reactions, neutron physics, and information technology. The institute has a division to study radiation and radiobiological research and other ad hoc experimental physics experiments. Principal research instruments include a nuclotron superconductive particle accelerator (particle energy: 7 GeV), three isochronic cyclotrons (120, 145, 650 MeV), a phasotron (680 MeV) and a synchrophasotron (4 GeV). The site has a neutron fast-pulse reactor (1500 MW pulse) with nineteen associated instruments receiving neutron beams.

Figure 1 Joint Institute for Nuclear Research

1.2 Flerov Laboratory of Nuclear Reactions - FLNR

Flerov Laboratory of Nuclear Reactions (FLNR), founded in 1957, is one of the eight departments of JINR. Research work in this department is known worldwide mainly due to the synthesis of new super heavy elements (and new isotopes of SHE), which in four cases received names in honour of this research facility: Dubnium (Z = 105, named after the city Dubna), Flerovium (Z = 114, named in honour of the Soviet nuclear physicist Georgy Flyorov), Moscovium (Z = 115, named after the Moscow region) and Oganesson (Z = 118, named in honour of Russian nuclear physicist Yuri Oganessian).

Figure 2 Flerov Laboratory of Nuclear Reactions

1.3 Super Heavy Elements - SHE

Super heavy elements, also known as transactinide elements, transactinides, or super-heavy elements, are the chemical elements with atomic number greater than 103. The super heavy elements are those beyond the actinides in the periodic table; the last actinide is lawrencium (103). By definition, super heavy elements are also transuranium elements, i.e. having atomic numbers greater than that of uranium (92). Glenn T. Seaborg first proposed the actinide concept, which led to the acceptance of the actinide series. He also proposed a transactinide series ranging from element 104 to 121 and a super actinide series approximately spanning elements 122 to 153 (although more recent work suggests the end of the super actinide series to occur at element 157 instead). The transactinide seaborgium was named in his honour.

Super heavy elements are radioactive and have only been obtained synthetically in laboratories. No macroscopic sample of any of these elements have ever been produced. Super heavy elements are all named after physicists and chemists or important locations involved in the synthesis of the elements. IUPAC defines an element to exist if its lifetime is longer than 10−14 second, which is the time it takes for the atom to form an electron cloud. The known super heavy elements form part of the 6 d and 7 p series in the periodic table. Except for rutherfordium and dubnium, even the longest-lasting isotopes of super heavy elements have half-lives of minutes or less. The element naming controversy involved elements 102–109. Some of these elements thus used systematic names for many years after their discovery was confirmed.

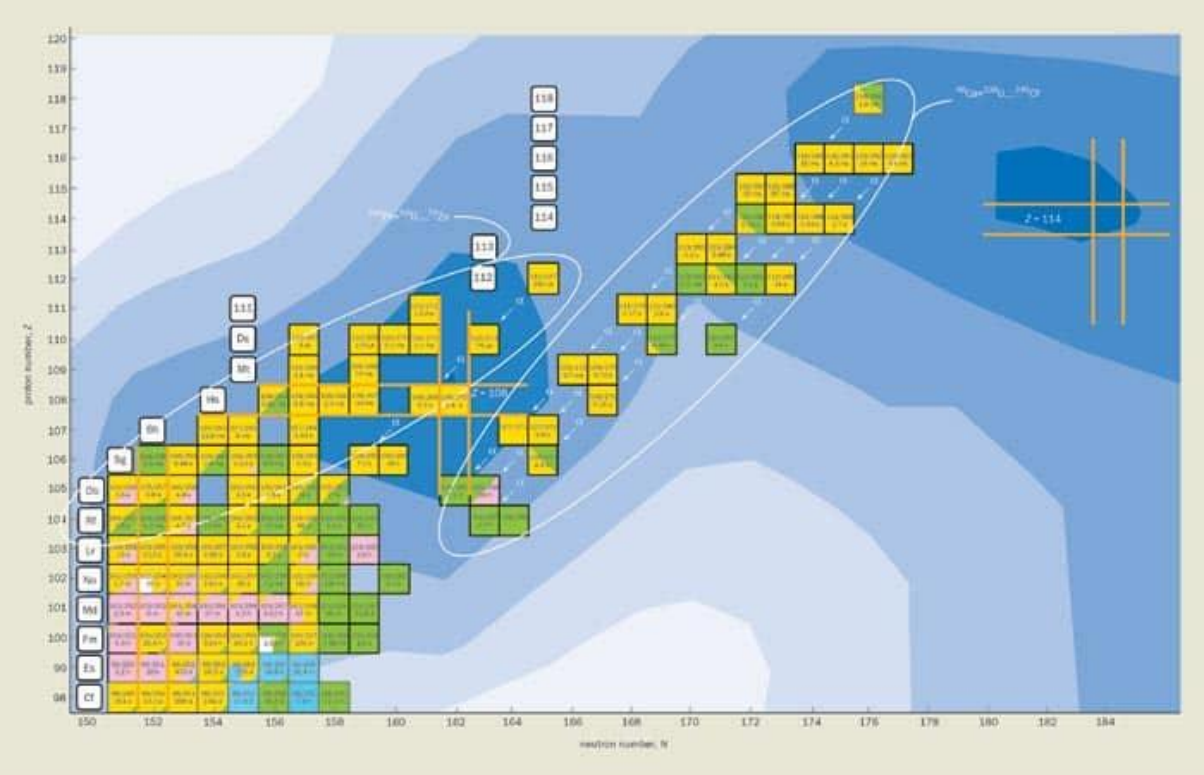

Figure 3 Super Heavy Elements

2. MASHA

2.1 Mass Analyser of Super Heavy Atoms - MASHA

Mass Analyser of Super Heavy Atoms (MASHA) is designed and manufactured for the purpose of identifying the mass of super heavy nuclei using mass spectrometry technology. The unique features of the mass separator are related to its ability to measure masses synthesized isotopes of super heavy elements and simultaneously record their α-decays and spontaneous fission. The MASHA installation consists of a target assembly with a hot catcher, an ion source based on the electron cyclotron resonance (ECR), a magneto-optical analyser (mass spectrometer) comprising four dipole magnets (D_1, D_2, D_{3a} and D_{3b}), three quadrupole lenses ($Q_{1,2,3}$) and two sextupole lenses (S_1, S_2). The detection system is located in the focal plane of the spectrometer.

Figure 4 MASHA

2.2 MASHA - Setup of the instrument

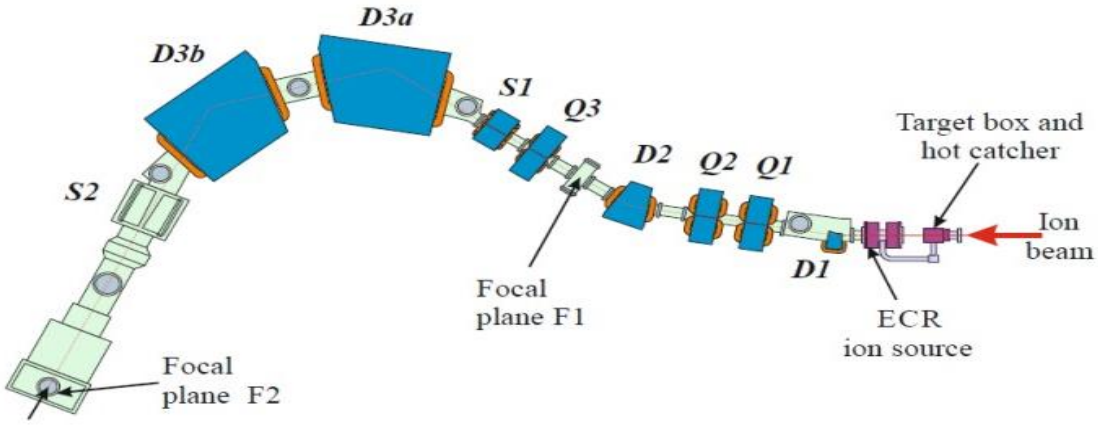

Figure 5 Schematic representation of the MASHA Setup with its main components.

2.2.1 Ion Source

In this part of the separator, the reaction products has been ionized with an ECR that contains a 2.45 GHz microwave oscillator. In the ion source, the atoms are ionized to charge state Q=+1. Then, these ions accelerated by the help of the electrode system and gathered into a beam. This beam is then separated with an optical system of the mass spectrometer. The efficiency of the ion source reaches 90% for the noble gases. Therefore, the ions that are in the current are almost 100% singly ionized.

2.2.2 Target Assembly and a Hot Catcher

When the ion beam enters this part, it incidents on a rotating target unit, consisting of 12 sectors, assembled in cassettes, revolving 25 rps via electric engine located right before the hot catcher unit. Prior to this collision, the energy and the intensity of the ion is being measured via pick-up detectors and a Faraday cups. After the collision, the injection of the fusion products to the ECR ion source takes place. Prior to this injection, fusion products hits on the pre-heated (up to 2000 K) graphite foil. Fusion products hit to the graphite to stop and cool down. While cooling down, ions fill their electron orbitals and diffuse through in the form of atoms into the vacuum of the hot catcher. From this, they move along a pipe and reach to the ECR ion source.

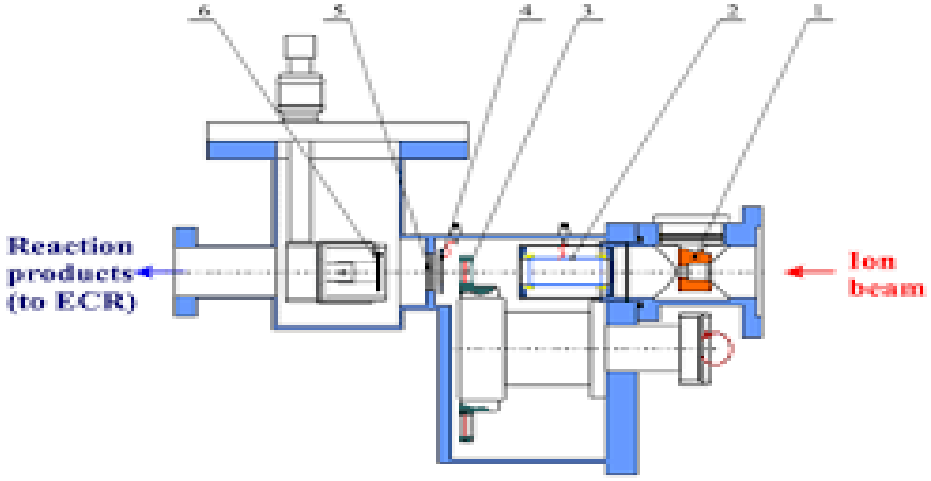

Figure 6 Schematic representation of Target assembly and Hot Catcher System 1–diaphragm; 2–pick-up sensor; 3–target on the wheel; 4–electron emission beam monitor; 5–separating foil; 6 – hot catcher

2.2.3 Detector

In order to detect the reaction products, a silicon strip detector system is used in the MASHA. In order to cover as much area as possible, the detector is a well-type detector that contains front, side and lateral detectors. The front detector consists of 192 strips with a 1.25 mm pitch. Side detectors on the other hand has 64 strips. The energy resolution of the detector is about 30 keV and It is possible to detect at least 90% of the decay products (α particles) if it occurs in the middle of the front detector.

The other detector in the system is TIMEPIX pixel detector and it is used for detecting the β^- and α particles. It is possible to detect even a single β^- and α particles with this detector together with the γ and X-rays. The detector consists of a full sensitive area of 14 x 14 mm^2 and has an array of 256 x 256 pixels on it.

Figure 7 Focal Plane silicon multi strip detector

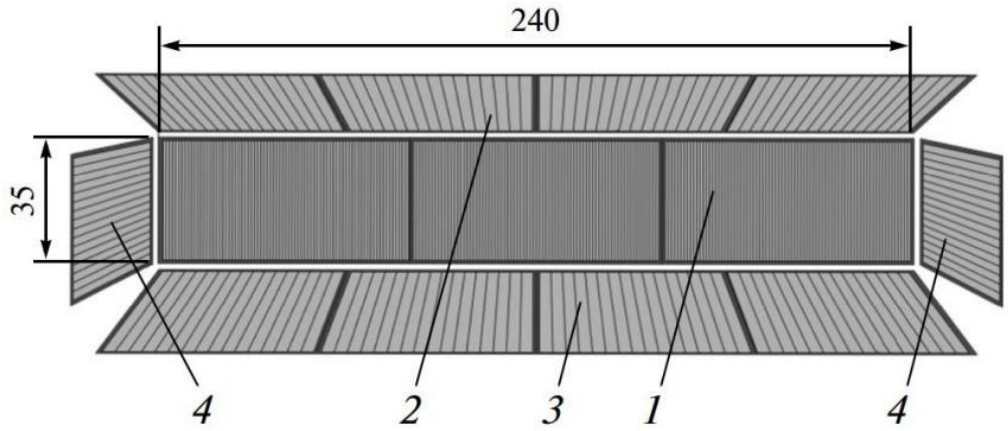

Figure 8 Detector system: 1- front detector; 2,3- side detectors; 4- lateral detectors

2.2.4 Data Acquisition System

The signals from the detectors are collected with independent spectrometric channels and then, routed to the data acquisition system consists of charge-sensitive preamplifier with 16 preamplifiers that are outside of the vacuum chamber. From these preamplifiers, the signals are directed to the 8-channel driver amplifiers with a built-in multiplexer. After these steps, three outputs are taken from the multiplexer: Alpha, fragment and digital channels. The digital channels contain the information on the source of the input signal and these outputs are connected to the XIA multi-channel high-speed digitizers.

3. Method of operation

The beam is accelerated with the U-400M cyclotron then goes through the target box then the not interacted beam and the reaction products are stopped by the hot catcher. The recoil nuclei that escape from the target layer stop in the graphite catcher at a depth of several micrometres. Due to the high temperature of the catcher, they diffuse into the ion source chamber, are extracted from the plasma with the help of three-electrode electrostatic lenses, accelerated by an electric field, and analysed by mass by magnetic fields as they move towards the detector. In this design, the mass of the atom can be determined with mass resolution of about M/dM = 1600. Since the reaction products tend to decay. Then the matrix of α-energies is formed by the number of strips. The strip number corresponds to the mass number.

MASHA was constructed at one of the beam outs of U-400M cyclotron in order to conduct online measurements of the physical properties of super heavy elements. The target was bombarded by beam of ^{48}Ca with energy E_{beam} = 7.3 MeV/n. The beam is stopped in the graphite catcher heated up to 1800 K. Atoms diffuse from the graphite volume and, move along the vacuum pipe and reach the ECR ion source discharge chamber where they are ionized. Faraday cup allows beam intensity control or target protection by periodically interrupting the beam. The separation efficiency and time were measured for Hg isotopes due to their similarity with element Z=112. α radioactive isotopes were obtained in the fusion reaction $^{40}Ar + ^{148}Sm \rightarrow ^{188-xn}Hg + xn$. α decay energy of the fusion products was measured as a function of the strip number. The full separation efficiency for the short-lived mercury isotopes was 7 % and the separation time was 1.8 s. Rn was obtained in the $^{40}Ar + ^{166}Er$ reaction and in the multinucleon transfer reaction $^{48}Ca + ^{242}Pu$, which also has a high cross section and used as a homologue of Cn.

The data were processed by OriginPro software environment, where data of the energy spectra of the α-decays were entered in the form of ASCII-tables. In this case, α-spectrum obtained isotopes were illustrated taking into account the evaporation of a certain number of neutrons from the excited compound nucleus.

4. Task

The task consists of plotting and analysing data from the detectors. Data is obtained from 3 different reactions. The decay energy is obtained along with alpha branching ratio and the identification of the isotopes. The strip detector has been calibrated and the results are showed on the heat map. This project aims to perform a mass measurement of short-lived isotopes of Hg (as the homologue to SHE), Rn and its daughter nuclei by α-decay chains at position sensitive Si detector and Simultaneous yield measurements of Cn, Fl and Hg.

4.1 Discussion

The reactions that will be discussed are the following:

i) Fusion reaction: $^{40}Ar + {}^{148}Sm \rightarrow {}^{188\text{-}xn}Hg + xn$

ii) Fusion reaction: $^{40}Ar + {}^{166}Er \rightarrow {}^{206\text{-}xn}Rn + xn$

iii) Multineutron reaction: $^{48}Ca + {}^{242}Pu \rightarrow {}^{21x}Rn$

4.1.1 Argon - 40 beam and Samarium - 148 target

$^{148}Sm_{62}$ ($^{40}Ar_{18}$; 3n) $^{185}Hg_{80}$……(1a)

$^{148}Sm_{62}$ ($^{40}Ar_{18}$; 4n) $^{184}Hg_{80}$……(1b)

$^{148}Sm_{62}$ ($^{40}Ar_{18}$; 5n) $^{183}Hg_{80}$……(1c)

$^{148}Sm_{62}$ ($^{40}Ar_{18}$; 6n) $^{182}Hg_{80}$……(1d)

$^{148}Sm_{62}$ ($^{40}Ar_{18}$; 7n) $^{181}Hg_{80}$……(1e)

$^{148}Sm_{62}$ ($^{40}Ar_{18}$; 8n) $^{180}Hg_{80}$……(1f)

$^{185}Hg_{80}$ (as a reaction product 1a): 94 % ε, 6 % α, $T_{1/2}$ = 49.1 s

$^{184}Hg_{80}$ (as a reaction product 1b): 98.89 % ε, 1.11 % α, $T_{1/2}$ = 30.87 s

$^{183}Hg_{80}$ (as a reaction product 1c): 88.3 % ε, 11.7 % α, $2.6 \cdot 10^{-4}$ % ε p, $T_{1/2}$ = 9.4 s

$^{182}Hg_{80}$ (as a reaction product 1d): 86.2 % ε, 13.8 % α, $T_{1/2}$ = 10.83 s

$^{181}Hg_{80}$ (as a reaction product 1e): 73 % ε, 27 % α, 2.6 · 0.01 % ε p, $T_{1/2}$ = 3.6 s

$^{180}Hg_{80}$ (as a reaction product 1f): 52 % ε, 48 % α, $T_{1/2}$ = 2.59 s

4.1.2 Argon-40 beam and Erbium-166 target

$^{166}Er_{68}$ ($^{40}Ar_{18}$; 1n) $^{205}Rn_{86}$ ……(2a)

$^{166}Er_{68}$ ($^{40}Ar_{18}$; 2n) $^{204}Rn_{86}$ …… (2b)

$^{166}Er_{68}$ ($^{40}Ar_{18}$; 3n) $^{203}Rn_{86}$…… (2c)

$^{166}Er_{68}$ ($^{40}Ar_{18}$; 4n) $^{202}Rn_{86}$ …… (2d)

$^{166}Er_{68}$ ($^{40}Ar_{18}$; 5n) $^{201}Rn_{86}$ …… (2e)

$^{205}Rn_{86}$ (as a reaction product 2a): 75.4 % ε, 24.6 % α, $T_{1/2}$ = 170 s

$^{204}Rn_{86}$ (as a reaction product 2b): 72.4 % α, 27.6 % ε, $T_{1/2}$ = 74.5 s

$^{203}Rn_{86}$ (as a reaction product 2c): 66 % α, 34 % ε, $T_{1/2}$ = 44 s

$^{202}Rn_{86}$ (as a reaction product 2d): 78 % α, 22 % ε, $T_{1/2}$ = 9.7 s

$^{201}Rn_{86}$ (as a reaction product 2e): ? α, ? ε, $T_{1/2}$ = 7 s

4.1.3 Calcium-48 beam and Plutonium-242 target

Due to the high excitation energies of such compound nuclei formed by reactions, de excitation is not only possible by neutron emission, but by larger nuclei that are not directly identifiable. Only the resulting products can be identified.

$^{242}Pu_{94}$ ($^{48}Ca_{20}$; multi-nucleon transfer) $^{219}Rn_{86}$ ……(3a)

$^{242}Pu_{94}$($^{48}Ca_{20}$; multi-nucleon transfer) $^{218}Rn_{86}$…… (3b)

$^{242}Pu_{94}$($^{48}Ca_{20}$; multi-nucleon transfer) $^{212}Rn_{86}$ …… (3c)

$^{219}Rn_{86}$(as a reaction product 3a): 100 % α, $T_{1/2}$ = 3.96 s

$^{218}Rn_{86}$(as a reaction product 3b): 100 % α, $T_{1/2}$ = 35 ms

$^{212}Rn_{86}$(as a reaction product 3c): 100 % α, $T_{1/2}$ = 23.9 min

5. Detailed Discussions and Results

5.1 Argon - 40 beam and Samarium - 148 target

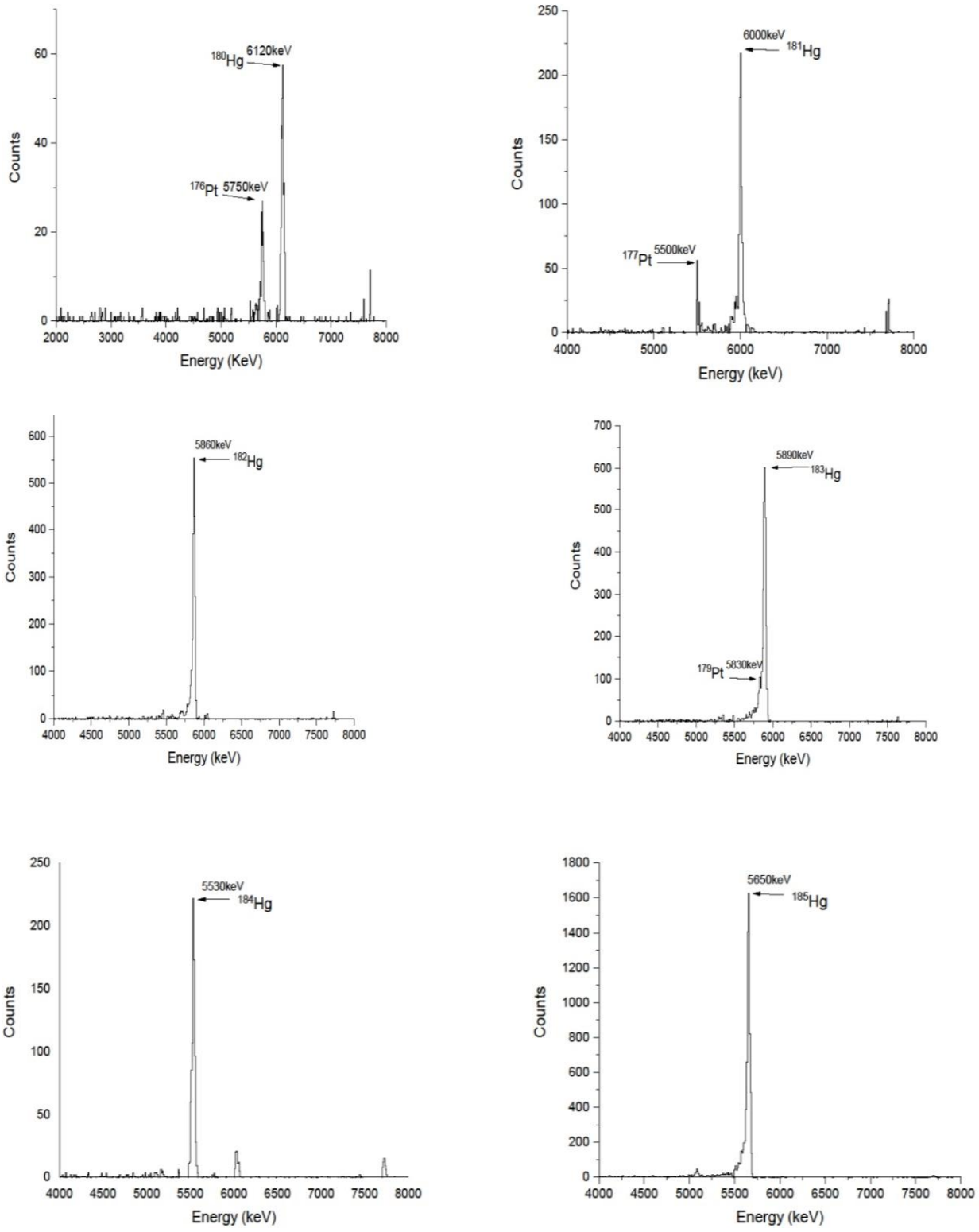

Figure 9 Energy Spectrum of the α – particles from decays of Hg

5.1.1 Explanation for the Spectrum obtained for Mercury

Spectrum 1 on the figure is experimentally measured spectrum for Hg-180 which is produced as described in equation 1f. There is a peak at energy 6120 keV which is a peak of Hg-180 with intensity of 47.9 %. Its daughter, Pt-176 (Hg-180 has 48 % probability of alpha decay), has the visible peak at energy 5750 keV with intensity 40 %. The other 52 % of decay probability is electron capture which comes to Au-180 whose decay (peaks) is not good known (98 % of Au-180 decays to Pt-180 which peak 5140 keV cannot be seen in spectrum because of low intensity 0.28 %). Furthermore, any other daughters of Pt-176 (Ir-176, Os-172, Os-176) are not recognizable in the spectrum. Peak with energy 7700 keV unfortunately cannot be identified. Due to the fact that this peak is more or less visible on all spectra, it is probably some background nuclide or pollution from previous experimental campaigns.

Spectrum 2 is experimentally measured spectrum for Hg-181 which is produced as described in equation 1e. There is a peak at energy 6000 keV which is a peak of Hg-181 with intensity of 21.4 %. Its daughter, Pt-177 (Hg-181 has 27 % probability of alpha decay), has the visible peak at energy 5500 keV.

Spectrum 3 is experimentally measured spectrum for Hg-182 which is produced as described in equation 1d. There is a peak at energy 5860 keV which is a peak of Hg-182 with intensity 15 %. It has 86 % probability to electron capture and 14 % to alpha decay. Daughter of Hg-182 electron capture is Au-182 whose peaks have a minimal intensity (about 0.1 %) and cannot be seen in spectres. The product of Hg-182 alpha decay is Pt-178 with an important peak at energy 5450 keV with intensity 4 % which is next to big peak. Peak at energy about 7700 keV is also easily recognizable but cannot be identified (see above).

Spectrum 4 is experimentally measured spectrum for Hg-183 which is produced as described in equation 1c. The main peak for this nuclide is at energy 5890 keV with intensity 11 % which come from alpha decay. Peak 5195 keV (with intensity 0.24 %) which belongs to the daughter Pt-179, was not measured. Likewise, no other daughters or their peaks were observed. Peak with energy about 7700 keV is also easily recognizable but cannot be identified (see above).

Spectrum 5 is experimentally measured spectrum for Hg-184 which is produced as described in equation 1b. The main peak for this nuclide is at energy 5530 keV with intensity 1.25 % which come from alpha decay. Other peaks of this nuclide have an intensity about 0.005 % which is too low to observe. Unfortunately, the

peak at energy 6030 keV cannot be identified - the vast majority of daughters are transformed exclusively by electron capture, and the intensities of individual peaks of partial alpha transformation are not sufficiently represented to form such a large peak. Thus, the sample may have been contaminated, or other unexpected radionuclides may have formed.

Spectrum 6 is experimentally measured spectrum for Hg-185 which is produced as described in equation 1a. The main peak for this nuclide is at energy 5650 keV with intensity 5.8 % which come from alpha decay. The other recognised peak is at energy 5080 keV (intensity 0.26 %) which belongs to Au-185. This radionuclide is made through electron capture from Hg-185. No other peaks were visible in the spectrum.

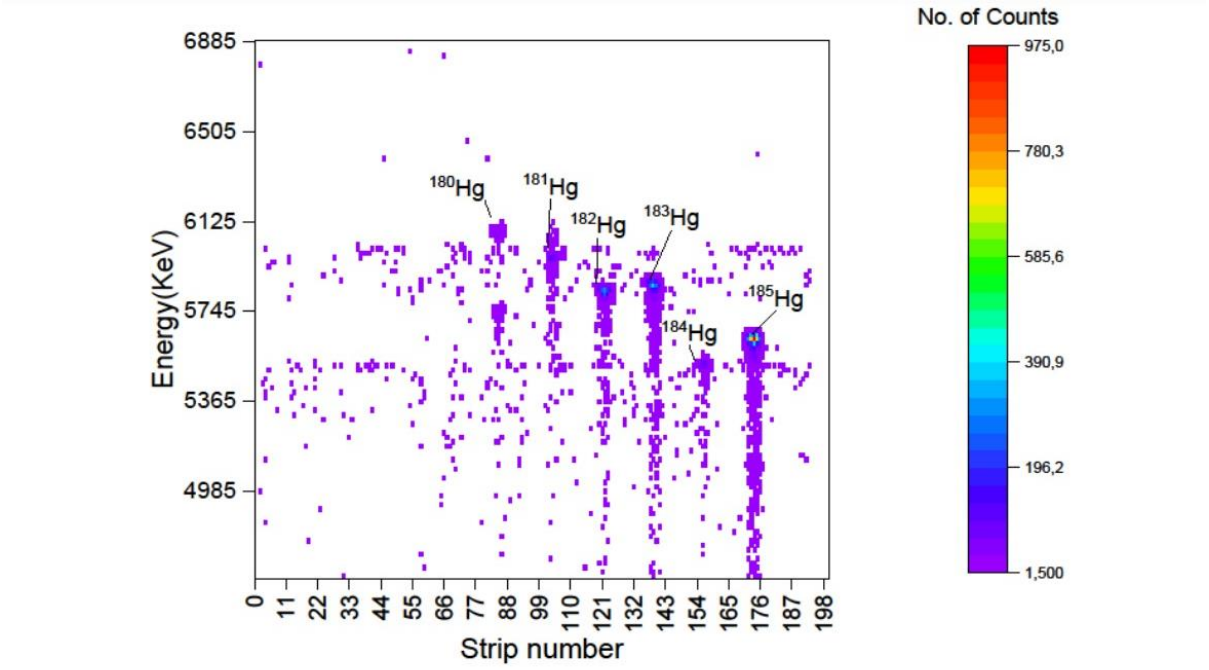

Figure 10 Energy and strip number plot of the α – particles from the decays of mercury isotopes

Heatmap on the above figure symbolizes the counts of gained mercury radionuclides depending on the energy (the energy values had to be calibrated before plotting on the heatmap, according to the instructions from the supervisor).

5.1.2 Comparison between the theoretical and experimental values of the energies for reaction between ^{40}Ar and ^{148}Sm with error percentage.

Table 1

Isotope	$T_{1/2}$(s)	Energy experiments (keV)	Energy Theoretical (keV)	Percentage Error
^{176}Pt	6.33	5750	5884	2.27
^{177}Pt	10	5500	5642	2.51
^{179}Pt	21.2	5830	5814	0.28
^{180}Hg	2.59	6120	6258	2.20
^{181}Hg	3.6	6000	5996	4.51
^{182}Hg	10.83	5860	6284	2.26
^{183}Hg	9.4	5890	6039	2.46
^{184}Hg	30.87	5530	5660	2.29
^{185}Hg	49.1	5650	5773	2.18

The **Branching Ratios (BR)** for the different isotopes are the following:

^{176}Pt (ec or $\beta^+ \rightarrow 60\%$, $\alpha \rightarrow 40\%$)

^{177}Pt (ec or $\beta^+ \rightarrow 94.3\%$, $\alpha \rightarrow 5.7\%$)

^{179}Pt (ec or $\beta^+ \rightarrow 99.76\%$, $\alpha \rightarrow 0.24\%$)

^{180}Hg (ec or $\beta^+ \rightarrow 52\%$, $\alpha \rightarrow 48\%$)

^{181}Hg (ec or $\beta \rightarrow 73\%$, $\alpha \rightarrow 27\%$)

^{182}Hg (ec or $\beta \rightarrow 86.2\%$, $\alpha \rightarrow 13.8\%$)

^{183}Hg (ec or $\beta \rightarrow 88.3\%$, $\alpha \rightarrow 11.7\%$)

^{184}Hg (ec or $\beta \rightarrow 98.89\%$, $\alpha \rightarrow 1.11\%$)

^{185}Hg (ec or $\beta \rightarrow 94\%$, $\alpha \rightarrow 6\%$)

5.2 Argon-40 beam and Erbium-166 target

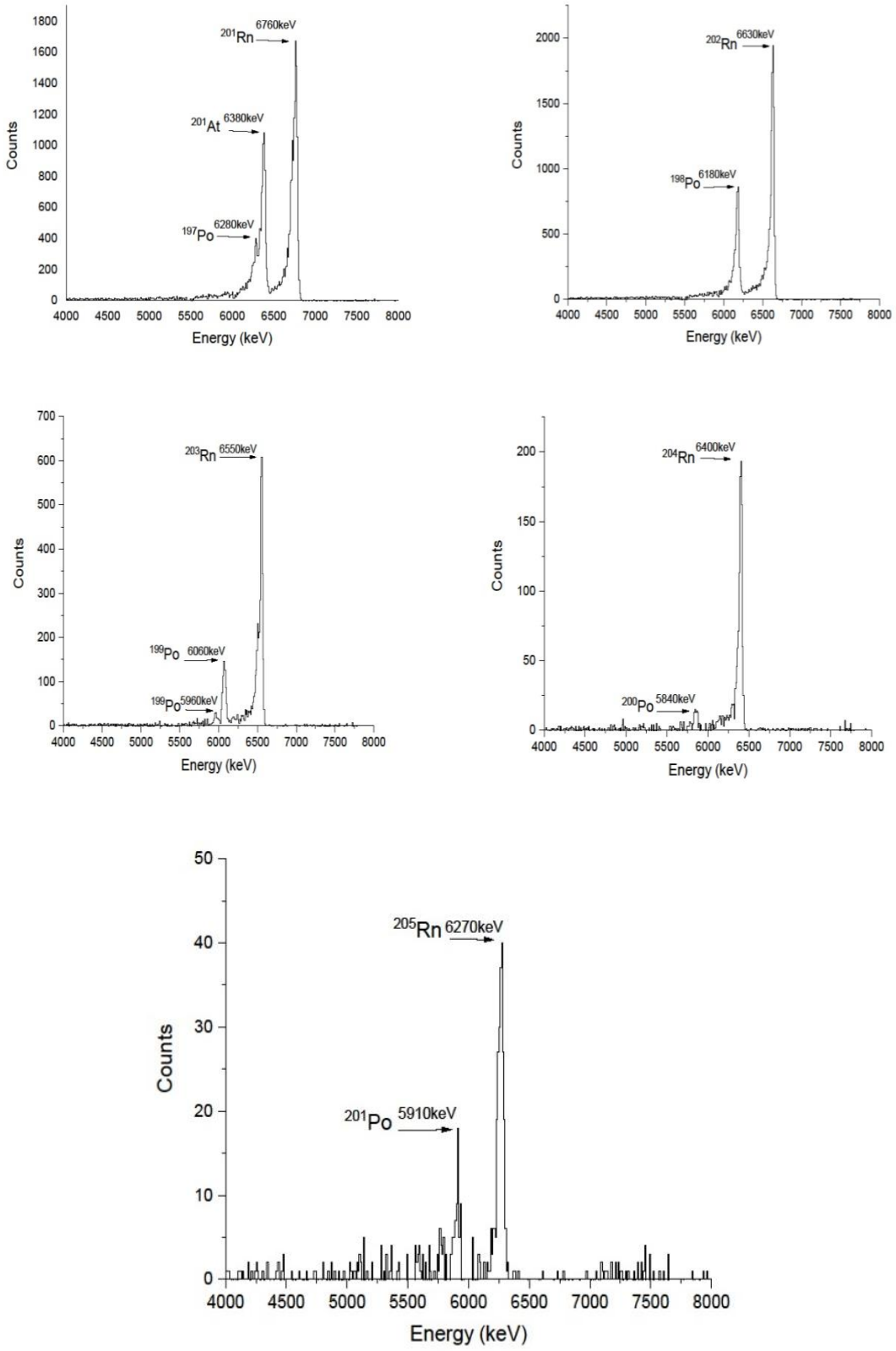

Figure 11Energy Spectrum of the α – particles from decays of Rn

5.2.1 Explanation for the Spectrum obtained for Radon

Spectrum 1 is experimentally measured spectrum for Rn-201 which is produced as described in equation 2e. The highest peak (with 1674 counts) belongs to Rn-201 with intensity 90 %. The other big peak probably comes from its daughter - At-201 which is made through electron capture. The tabulated value of this peak is 6342 keV, and this peak in the spectrum has 6380 keV. Due to the high intensity of the astatine peak, the high counts of the peak in the spectrum, and the relatively high probability of the formation of this nuclide, this difference in energy was neglected and the given peak was assigned to the astatine. The parasitic peak on the left side of the At-201 peak (with an energy of 6281 keV) was identified as the Po-197 peak (with an intensity of 59 %). This radionuclide Po-197 is the daughter of At-201 transformed by alpha conversion. An unidentified peak with an energy of approximately 7700 keV, which was noticeable on the previous spectra, now only turns into noise.

Spectrum 2 is experimentally measured spectrum for Rn-202 which is produced as described in equation 2d. The main peak at energy 6630 keV belongs to Rn-202 which has intensity about 78 %. The peak (at energy 6180 keV and intensity 58 %) is peak of Rn-202's alpha daughter - Po-198. No further peaks were detected in the spectrum.

Spectrum 3 is experimentally measured spectrum for Rn-203 which has a peak with energy 6550 keV and which is produced as described in equation 2c. It has 608 counts and intensity 75 %. The alpha daughter of Rn-203 is the metastable Po-199m, which has a peak next to it at energy 6060 keV with intensity 39 %. The ground state of this radionuclide is then also visible in the spectrum, in the form of a slightly overlooked peak at an energy of 5960 keV with intensity 12 %. Any additional peaks of other radon radionuclide daughters are indistinguishable from detector and background noise.

Spectrum 4 is experimentally measured spectrum for Rn-204 which is produced as described in equation 2b. The dominant peak in this spectrum is the peak at an energy of 6400 keV, which can be assigned to the radionuclide Rn-204. The tabulated value of this peak is 18 keV higher, but due to the high intensity (100 %) there is a high probability of misidentification. The second identified peak is the peak at an energy of 5840 keV, which belongs to the alpha daughter Rn-204, namely, the Po-200 with an intensity of 11 %. Due to the fact that even in this

case the tabulated peak value is about 21 keV higher, there is a probability of incorrect calibration of the detector. Peak at an energy value of about 7700 keV is again visible on this spectrum, but unfortunately it is still unidentifiable.

Spectrum 5 is experimentally measured spectrum for Rn-205 (which is produced as described in equation 2a) and it is the last spectrum for the argon-40 beam and erbium-166 target. It must be taken into account that the counts are an order of magnitude lower compared to the previous spectra, and in this case the effect of the background noise will be significantly more pronounced. Despite this difficulty, however, two peaks can be identified - the basic peak Rn-205 with an energy of 6270 keV (and intensity 24.2 %) and the peak of its daughter (created by electron capture) At-205 at an energy of 5910 keV (intensity 10 %).

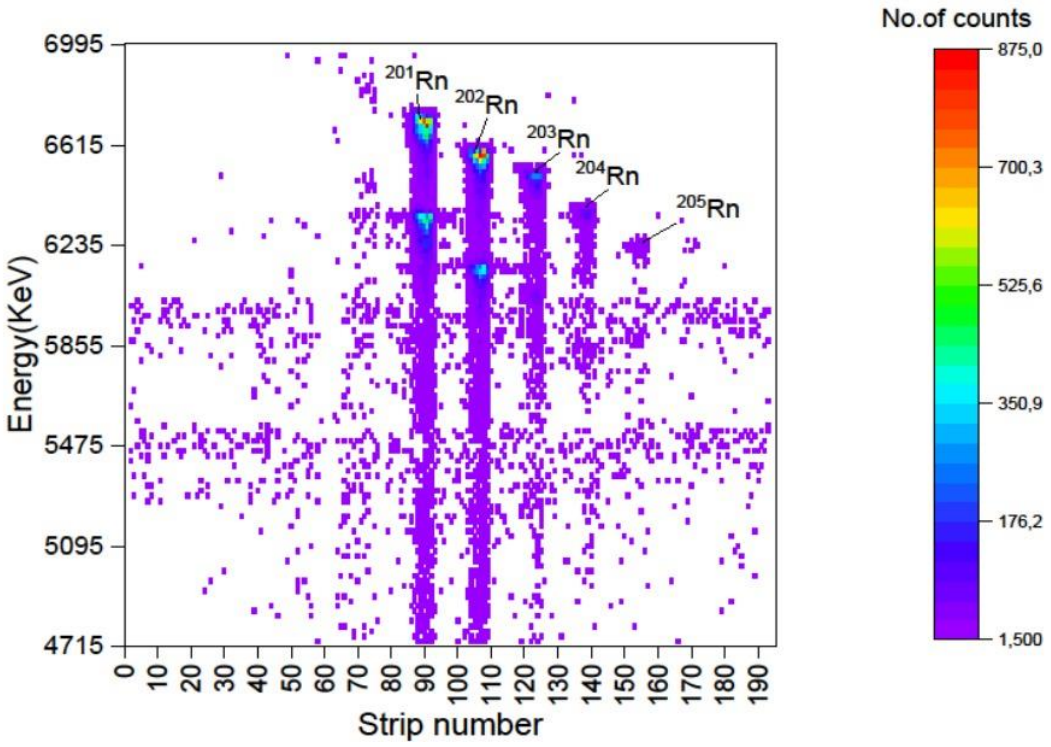

Figure 12 Energy and strip number plot of the α – particles from the decays of Radon isotopes

Heatmap on figure above symbolizes the counts of gained mercury radionuclides depending on the energy (calibrated energy values).

5.2.2 Comparison between theoretical and experimental values of energies for ^{40}Ar and ^{166}Er reaction with error percentage.

Table 2

Isotope	$T_{1/2}$(s)	Energy experiments (keV)	Energy Theoretical (keV)	Percentage Error
^{197}Po	53.6	6280	6411	2.04
^{198}Po	106.2	6180	6309	2.04
^{199}Po	328	5060	6074	0.23
^{200}Po	691	5840	5981	2.35
^{201}Po	919	5910	5799	1.91
^{201}At	85.2	6380	6472	1.42
^{201}Rn	7	6760	6860	1.45
^{202}Rn	9.94	6630	6773	2.15
^{203}Rn	44.2	6550	6630	1.20
^{204}Rn	70.2	6400	6546	2.23
^{205}Rn	170	6270	6386	1.81

The **Branching Ratios (BR)** for the following isotopes are:

^{197}Po (ec or $\beta^+ \rightarrow$ 56%, $\alpha \rightarrow$ 44%)

^{198}Po (ec or $\beta^+ \rightarrow$ 57%, $\alpha \rightarrow$ 43%)

^{199}Po (ec or $\beta^+ \rightarrow$ 92.5%, $\alpha \rightarrow$ 7.5%)

^{200}Po (ec or $\beta^+ \rightarrow$ 88.9%, $\alpha \rightarrow$ 11.1%)

^{201}Po (ec or $\beta^+ \rightarrow$ 98.87%, $\alpha \rightarrow$ 1.13%)

^{201}At (ec or $\beta^+ \rightarrow$ 29%, $\alpha \rightarrow$ 71%)

^{201}Rn (ec or $\beta^+ \rightarrow$?, $\alpha \rightarrow$?)

^{202}Rn (ec or $\beta^+ \rightarrow$22%, $\alpha \rightarrow$ 78%)

^{203}Rn (ec or $\beta^+ \rightarrow$ 34%, $\alpha \rightarrow$ 66%)

^{204}Rn (ec or $\beta^+ \rightarrow$ 27.6%, $\alpha \rightarrow$ 72.4%)

^{205}Rn (ec or $\beta^+ \rightarrow$ 75.4%, $\alpha \rightarrow$ 24.6%)

5.3 Calcium-48 beam and Plutonium-242 target

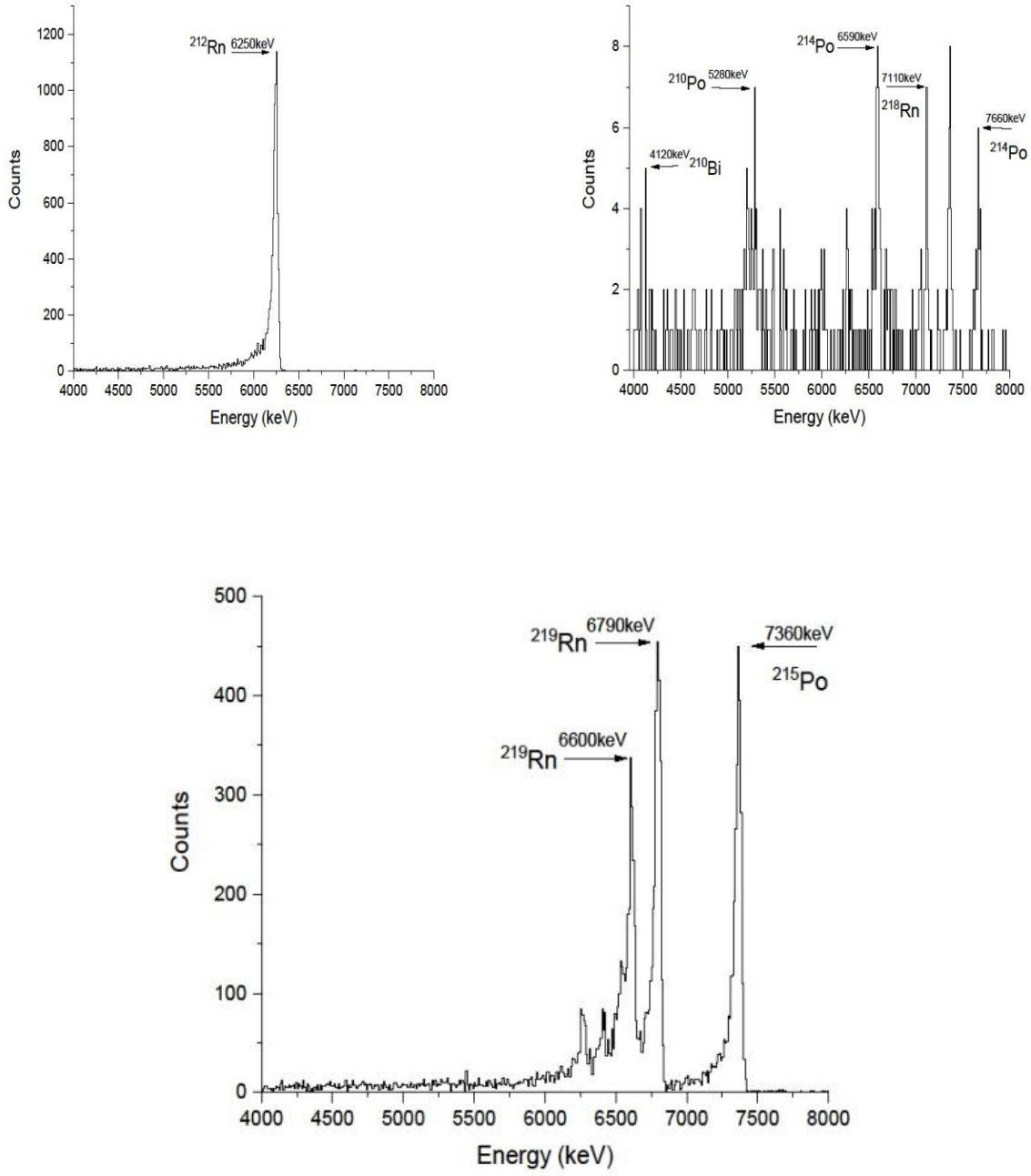

Figure 13 Energy and strip number plot of the α – particles from the decays of Radon isotopes

5.3.1 Explanation for the Spectrum obtained for Radon

Spectrum 1 is experimentally measured spectrum for Rn-212 which is produced as described in equation 3c. This spectrum has significantly higher counts than the spectra obtained for other radionuclides in this experimental campaign (see figures 10b and 11). For this reason, the identification of peaks is much clearer. In this case, only one peak belonging to Rn-212 was identified (energy 6250 keV, 1139 counts, intensity 99.95 %). The alpha daughter of the radionuclide Rn-212 is Po-208 with a major peak around 5115 keV. However, it is not visible on the spectrum, due to the large half-life, which is almost 3 years, and during a short measurement, a sufficient number of counts is not recorded.

Spectrum 2 is experimentally measured spectrum for Rn-219 which is produced as described in equation 3a. A large number of peaks and radionuclides were identified in this spectrum (despite relatively low counts). The main peak Rn-219 was found to be 6790 keV (with an intensity of 79.4 %; tabulated value 6819 keV). Secondary, less visible but identifiable peaks of the same radionuclide are the peaks at 6400 keV (intensity 7.5 %, tabulated value 6425 keV) and 6530 keV (intensity 12.9 %, tabulated value 6553 keV, parasitic at the peak with energy 6600 keV). The alpha daughter of the radionuclide Rn-219 is the radionuclide Po-215, which is visible at the peak with an energy of 7360 keV (intensity almost 100 %, tabulated energy 7386 keV). The third radionuclide identified is Bi-211, which was identified by a main energy peak of 6600 keV (intensity 83.54 %, tabulated value 6623 keV) and a secondary energy peak of 6250 keV (intensity 16.19 %, tabulated value 6278 keV). However, the mechanism of formation of this radionuclide is not the alpha of Po-215, as it might seem, but in a more complicated, but realistic way:

$^{219}Rn_{86} \rightarrow 100\ \%\ \alpha;\ T_{1/2} = 3.96\ s \rightarrow {}^{215}Po_{84} \rightarrow 100\ \%\ \alpha\ ;\ T_{1/2} = 1781\ \mu s \rightarrow {}^{211}Pb_{82}$
$\rightarrow 100\ \%\ \beta^-\ ;\ T_{1/2} = 36.1\ min \rightarrow {}^{211}Bi_{83}$ (99.72 % ; $T_{1/2} = 2.14$ min)

There is also the possibility of contamination of the spectrum by naturally occurring radionuclides, as the resulting Rn-219, Po-215, Pb-211, and Bi-211 are part of a naturally occurring actinium decay series. Due to more or less the same deviations of the experimental from the tabulated energy values, it is reasonable to consider a poor calibration of the detector, which should be solved in further experiments.

Spectrum 3 is experimentally measured spectrum for Rn-218 which is produced as described in equation 3b. Unfortunately, due to the really low activities,

which are only in the order of units of counts, the search and identification of peaks were very difficult and there is a great possibility for errors. There is also the possibility of contamination of the spectrum by naturally occurring radionuclides, as the resulting polonium Po-214 is part of a naturally occurring uranium radium decay series. Despite this fact, two of the peaks were identified. First peak with an energy of 7666 keV, which was assigned to the radionuclide Po-214 (intensity almost 100 %, tabulated energy 7687 keV). This radionuclide is the direct alpha daughter of Rn-218. The second peak is at energy 5287 keV and it was identified as Po-210 (intensity 100 %; tabulated energy 5304 keV). The mechanism of formation of this radionuclide is more complex (and may not be correct), but it can be, from my point of view, realistic:

$^{218}Rn_{86} \rightarrow$ 100 % α; $T_{1/2}$ = 35 ms $\rightarrow {}^{214}Po_{84} \rightarrow$ 100 % α ; $T_{1/2}$ = 164 µs $\rightarrow {}^{210}Pb_{82}$ $\rightarrow$100 % β^- ; $T_{1/2}$ = 22.2 y $\rightarrow {}^{210}Bi_{83}$ (100 % β^- ; $T_{1/2}$ = 5.012 d) $\rightarrow {}^{210}Po_{84}$ (100 % α ; $T_{1/2}$ = 138.376 d)

Other peaks were automatically detected by the Origin program in the spectrum, but it is very likely that they are random peaks caused by detector noise and background noise.

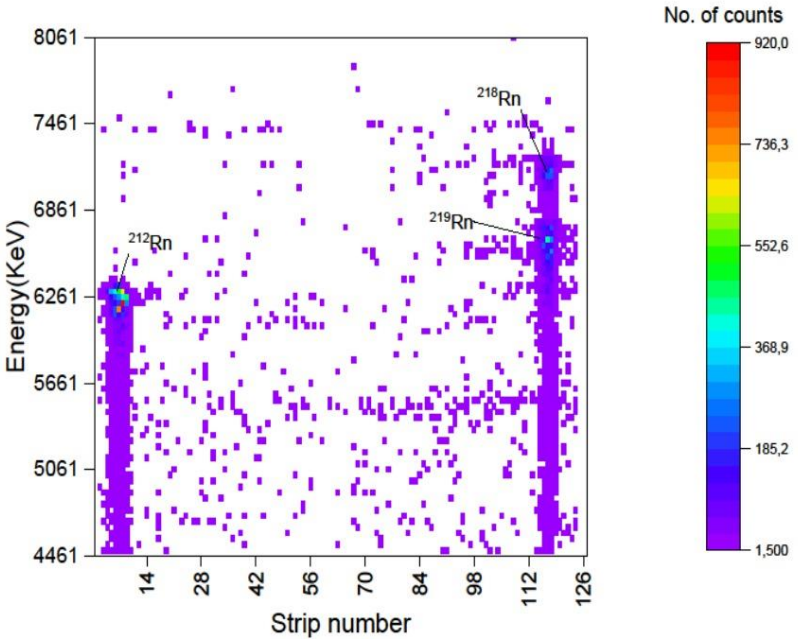

Figure 14 Energy and strip number plot of the α – particles from the decays of Radon isotopes

Heatmap on figure above symbolizes the counts of gained mercury radionuclides depending on the energy with calibrated values. The fact that even on this heatmap no trace of the radionuclide Rn-218 is visible only confirms

the description of figure 11 that the peaks of the radionuclides obtained are not so visible that they can be unambiguously separated from the noise.

5.3.2 Comparison between theoretical and experimental values of energies for ^{48}Ca and ^{242}Pu reaction with error percentage.

Table 3

Isotope	$T_{1/2}$(s)	Energy experiments (keV)	Energy Theoretical (keV)	Percentage Error
^{210}Bi	442368	4120	4100	0.48
^{210}Po	11955686	5280	5407	2.34
^{212}Rn	1434	6250	6385	2.11
^{214}Po	0.00016346	7660	7833	2.20
^{215}Po	0.001781	7360	7526	2.20
^{218}Rn	0.03375	7110	7262	2.10
^{219}Rn	3.96	6790	6946	2.24

The **Branching Ratios (BR)** for these isotopes are the following:

^{210}Bi ($\beta^- \rightarrow 100\%$, $\alpha \rightarrow 13.2 \cdot 10^{-5}\%$)

^{210}Po (ec or $\beta^+ \rightarrow 0\%$, $\alpha \rightarrow 100\%$)

^{212}Rn (ec or $\beta^+ \rightarrow 0\%$, $\alpha \rightarrow 100\%$)

^{214}Po (ec or $\beta^+ \rightarrow 0\%$, $\alpha \rightarrow 100\%$)

^{215}Po ($\beta^- \rightarrow 2.3 \cdot 10^{-4}\%$, $\alpha \rightarrow 99.99977\%$)

^{218}Rn (ec or $\beta^+ \rightarrow 0\%$, $\alpha \rightarrow 100\%$)

^{219}Rn (ec or $\beta^+ \rightarrow 0\%$, $\alpha \rightarrow 100\%$)

6. Conclusion

The mass-separator MASHA was constructed to identify the super heavy elements by their mass-to-charge ratio and getting additional details by using the detector system. In the focal plane of the silicon detector, products of the above given complete fusion reactions and multi-nucleon transfer reactions were detected. α-spectra of the evaporative residues of the complete fusion reactions were analysed. Defined energies are well-matched with the values from the literature. The functionality of the apparatus and detection device was proved, but it decreases with increasing mass number and decreasing half-life. However, this is also related to the parameters of the accelerator, when it is necessary to expend higher energy for higher mass numbers and thus the assumption of a smaller number of cores. This increasing energy can also be seen in the presumed nuclear reactions, where compound nuclei need several neutrons ejected from lighter radionuclides for their de-excitation, while in the case of the hypothetical formation of flerovium, deexcitation is realized by ejection of larger nucleon units. Therefore, the basis of the follow-up research should be a better balance of the projectile's energy so that a complex nucleus is formed, but only with such energy that de-excitation can occur only by neutron ejection, or other simple particles, and the super heavy element nucleus. However, from the point of view of chemical properties, no further problem should arise, since the synionuclides synthesized should be chemically similar to the radionuclides of super heavy elements.

7. Acknowledgements

I would like to extend my heartfelt gratitude and thanks to the INTEREST team for giving me an opportunity along with a very amazing experience. I also put forward my gratitude to Mr. Vedeneev Viacheslav Yurievich, for guiding me and providing me with necessary information to complete this project, without whose help and guidance I wouldn't have been able to do this report. I would like to thank my professors, family, friends and others, who helped me in every smallest way possible to complete this project successfully.

References

1. Chemical identification of Dubnium as a decay product of element 115 produced in the reaction 48Ca + 243Am. S.N. Dmitriev, Yu.Ts. Oganessyan, V.K. Utyonkov et al. Dubnium as a decay product.

2. Chemical characterization of element 112. R. Eichler, N. V. Aksenov, A. V. Belozerov et al. Nature. Letters. Vol. 447, May 2007.

3. The current status of MASHA setup. V. Yu. Vedeneev, A.M. Rodin, L.Krupa. Hyperfine Interactions 238:19 (2017).

4. MASHA Separator on the Heavy Ion Beam for Determining Masses and Nuclear Physical Properties of Isotopes of Heavy and Superheavy Elements. A.M. Rodin, A.V. Belozerov, D.V. Vanin. Instruments and Experimental Techniques, 2014, Vol. 57, No. 4, pp. 386–393. © Pleiades Publishing, Ltd., 2014.

5. Gaggeler H. W. Mendeleev's principle against Einstein's relativity: news from the chemisrty of superheavy elements // Russian Chemical Reviews. — 2009. — Vol. 78, no. 12. — P. 1139–1144.

6. S. N. Dmitriev, Y. T. Oganessyan, V. K. Utyonkov, S. V. Shishkin, A. V. Yeremin, Y. V. Lobanov, Y. S. Tsyganov, V. I. Chepygin, E. A. Sokol, G. K. Vostokin, et al., "Chemical identification of dubnium as a decay product of element 115 produced in the reaction 48ca+ 243am," Mendeleev Communications, vol. 15, no. 1, pp. 1–4, 2005.

7. Abeer Attla, Lubos Krupa, and Aleksey Novoselov. Experimental data analysis at the MASHA setup. Dubna, 2016.

8. Meruyert Mamatova et al. "Study of production stability of radon and mercury isotopes in complete fusion reactions at the mass-separator MASHA by "solid hot catcher" technique". In: AIP Conference Proceedings 2163.1 (2019), p. 070002.